HHS Public Access

Author manuscript

J Magn Reson Imaging. Author manuscript; available in PMC 2021 September 01.

Published in final edited form as:

J Magn Reson Imaging. 2020 September ; 52(3): 864–872. doi:10.1002/jmri.27115.

Rotator Cuff Tendon Assessment in Symptomatic and Control Groups Using Quantitative Magnetic Resonance Imaging

Aria Ashir, B.S[1,2,3], **Yajun Ma, Ph.D.**[1], **Saeed Jerban, Ph.D.**[1], **Hyungseok Jang, Ph.D.**[1], **Zhao Wei, M.S.**[1], **Nicole Le, B.A.**[2], **Jiang Du, Ph.D.**[1], **Eric Y. Chang, M.D.**[2,1]

[1]Department of Radiology, University of California, San Diego, CA

[2]Research Service, VA San Diego Healthcare System, San Diego, CA

[3]College of Medicine, Drexel University, Philadelphia, PA

Abstract

Background: Relatively weak correlations between patient symptoms and rotator cuff tendon (RCT) tearing have been reported; however, the relationship between symptoms and tendinosis has been less well-studied.

Purpose/Hypothesis: To use quantitative MRI to assess the bilateral RCTs in shoulders of both patients with unilateral symptomatic tendinopathy and control subjects. We hypothesized that quantitative MRI measures would differ between symptomatic patients and controls.

Study Type: Prospective imaging study.

Population/Subjects: 48 shoulders from 24 subjects (mean age, 32.8 years), including 14 patients with unilateral symptomatic tendinopathy and 10 asymptomatic controls.

Field Strength/Sequence: 3T/3D Ultrashort Echo Time Cones sequence with magnetization transfer preparation (UTE-Cones-MT) and Carr–Purcell–Meiboom–Gill.

Assessment: Macromolecular fraction (MMF) and T_2 relaxation were measured in four regions of the superior RCT, including all-segments, and lateral-third, bursal-sided, and articular-sided segments. The Western Ontario Rotator Cuff (WORC) index and visual analog scale were assessed.

Statistical Tests: Three shoulder groups were evaluated, including symptomatic shoulders, contralateral asymptomatic shoulders in patients, and asymptomatic controls. MMF and T_2 values were compared between groups using a bootstrap-based comparison of means.

Results: Significant differences were found in both MMF and T_2 values between symptomatic and control RCTs when analyzing all-segments (p=0.027 and p=0.006, respectively) and articular-sided segments (both p=0.001). Significant differences between asymptomatic RCTs in patients and control RCTs were also found, including MMF in all four anatomic regions analyzed (p=0.024–0.044), as well as T_2 in all-segments (p=0.003), bursal-sided segments (p=0.021), and articular-sided segments (p=0.002). No significant differences in MMF (p=0.420–0.950) or T_2

Corresponding author: Eric Y. Chang, Radiology Service, VA San Diego Healthcare System, 3350 La Jolla Village Drive, San Diego, CA 92161, Phone: +1 858 642 1221, ericchangmd@gmail.com.

(p=0.380–0.910) were seen between ipsilateral symptomatic and contralateral asymptomatic RCTs in patients.

Data Conclusion: Symptomatic RCTs showed significantly lower MMF values and higher T_2 values compared with control RCTs. In patients with unilateral symptomatic tendinopathy, the contralateral shoulder can demonstrate asymptomatic tendinopathy which can be quantified using MMF or T_2.

Keywords

quantitative MRI; ultrashort echo time; magnetization transfer; T2; rotator cuff tendinopathy

Introduction

The primary dynamic stabilizer of the glenohumeral joint is the rotator cuff tendon (RCT) (1). RCT dysfunction can lead to abnormal joint kinematics through loss of force couples, deterioration of shoulder function, and ultimately cartilage degeneration and cuff arthropathy (1). RCT pathology is common, with an estimated 65–70% of all shoulder pain attributed to rotator cuff disease (2). However, many studies have also shown that chronic RCT tears may be asymptomatic (3,4). In fact, the prevalence of asymptomatic partial-thickness and full-thickness RCT tears is estimated to be up to 40% and 46%, respectively (5).

Although several studies have assessed the relationship between symptoms and RCT tears, the relationship between symptoms and tendinosis has been less well-studied. One limitation has been the difficulty in quantifying tendinosis. While conventional qualitative magnetic resonance imaging (MRI) is widely considered the non-invasive gold standard for evaluating RCT tears, it performs less well in the assessment of tendinosis. On clinical MRI, tendinosis is characterized by diffuse signal increase on low to intermediate echo time (TE) sequences with signal less than water on T_2-weighted images (6). However, Neumann et al. found that 89% of supraspinatus tendons in young, asymptomatic volunteers demonstrated this finding, which we now know can represent a normal tendon, degeneration, or magic angle artifact (7). Not surprisingly, other studies have reported the sensitivity of conventional MRI for the diagnosis of tendinosis to range from 13–79% and interobserver reliability to range from exceedingly poor (kappa values 0.14–0.27) (8,9) to moderate (intraclass correlation 0.55) (10).

Quantitative MRI techniques have been used to overcome some of these limitations, including measurement of T_2 / T_2* relaxation (11–13). However, transverse relaxation measurements are sensitive to the magic angle effect, with RCTs demonstrating up to a 100% increase in T_2 on an *ex vivo* study (14). More recently, ultrashort echo time (UTE) sequences have been shown to be useful for tendon evaluation (15). Up to 9% of supraspinatus tendons may demonstrate a signal void on images produced using TEs as short as 10 ms (7). With these and other short T_2 tissues, UTE sequences are particularly well suited for quantification. In particular, the UTE Cones magnetization transfer (UTE-Cones-MT) sequence with two-pool modeling analysis has been shown to be resistant to the magic angle effect, while maintaining the ability to distinguish between histologically normal and abnormal tendons (14).

Thus the purpose of this study was to use quantitative MRI to assess the bilateral RCTs in shoulders of both patients with unilateral symptomatic tendinopathy and control subjects. We hypothesized that quantitative MRI measures would differ between symptomatic patients and control subjects.

Materials and Methods

This study was approved by our institutional review board and all subjects provided and signed a statement of informed consent.

Study Population

Between July 2018 and April 2019, all patients presenting to our radiology department for a shoulder MRI exam were screened. Inclusion criteria included the following: clinical concern for RCT pathology as documented on the exam requisition, age between 18–45 years old, unilateral shoulder pain, and absence of both RCT tearing and non-RCT pathology on the clinical MRI exam of the symptomatic shoulder. Specifically, patients reporting bilateral shoulder pain at presentation or demonstrating acromioclavicular joint, bursal, labral, biceps-related, and/or glenohumeral osteochondral pathology on the clinical MRI exam were excluded. A board-certified musculoskeletal radiologist (E.Y.C., nine years of experience) confirmed subject eligibility based on coronal-oblique T_2-weighted fat-suppressed images obtained from the clinical MRI exam. In addition, ten healthy volunteers between 18–45 years old without shoulder pain were recruited as control subjects. Subjects that met inclusion criteria were invited to participate. All participants completed the Western Ontario Rotator Cuff (WORC) index (16), the visual analog scale (VAS), and underwent quantitative MRI examination of both shoulders.

MRI Protocol

Imaging was performed on a 3T clinical MRI scanner (MR750, GE Healthcare, Milwaukee, WI) using a four-channel shoulder coil. Patient shoulders were physically externally rotated and a coronal-oblique imaging plane was used. The 3D UTE-Cones-MT sequence employed an MT preparation followed by multiple 3D UTE-Cones interleaves to accelerate data acquisition (17). Specifically, this sequence uses a unique k-space trajectory that samples data along evenly spaced twisting paths in the shape of multiple cones (18). The MT preparation consisted of a Fermi-shaped radiofrequency (RF) pulse (duration = 8 msec, bandwidth = 160 Hz) followed by a gradient crusher. The 3D UTE-MT imaging parameters included: repetition time (TR) = 105 msec, echo time (TE) = 32 μs; flip angle (FA) = 7°; bandwidth (BW) = 125 kHz; field of view (FOV) = 17 cm; reconstruction matrix = 192 × 192; slice thickness = 3 mm; 20 slices; nine interleaves per MT preparation pulse; three MT powers (300°, 550°, 750°), and five MT frequency offsets (2, 5, 10, 20, 50 kHz) for a total of 15 different MT datasets, and a total scan time of 10 minutes. T_1 was measured with the combined actual flip angle and variable flip angle techniques with 3D UTE-Cones acquisition (3D UTE-AFI-VFA) on the same plane and spatial resolution, with other imaging parameters including (19,20): TRs = 20 and 100 ms; TE = 32 μs; FA = 5, 10, 20, and 30°; bandwidth = 125 kHz; and a total scan time of 9 minutes. A multi-slice 2D Carr–Purcell–Meiboom–Gill (CPMG) sequence was used for T_2 measurement with imaging

parameters including: TR = 800 ms, TEs = 7.9, 15.8, 23.7, 31.6, 39.5, 47.4, 55.3, 63.2 ms; FOV = 8 cm; acquisition matrix = 256 × 192; slice thickness = 3 mm; slice space = 0.6 mm; bandwidth = 32.5 kHz; and a total scan time of 5 minutes.

Clinical Symptoms Analysis

All symptomatic patients completed the Western Ontario Rotator Cuff (WORC) index for their problematic shoulder. The WORC is a disease-specific quality of life measurement tool for patients with rotator cuff disease which considers multiple categories related to shoulder pain and functionality including physical symptoms, sports/recreational activities, work activities, lifestyle, and emotional impact. The total WORC score is summarized into a percentage of normal shoulder function (16,21). In addition, all research subjects completed the visual analog scale (VAS) for both shoulders, which assesses general pain symptom severity from a scale of 0–10 (0–100 mm, no pain to worst pain).

MRI Analysis

All images were registered using a 3D nonrigid registration algorithm (elastix), carried out via the Insight Segmentation and Registration Toolkit (ITK) (22). In this study, 3D UTE-AFI-VFA images with TR = 20 ms and FA = 5° were treated as the fixed images and the remaining data sets were treated as images with potential motion. In the 3D non-rigid registration, both rigid (affine) and non-rigid (B-spline) algorithms were applied as a two-staged approach, driven by Advanced Mattes mutual information (23). The transformations were obtained by registration of the grayscale images, then applied to the labeled images. Adaptive stochastic gradient descent optimizer was used to optimize both the affine and B-spline registration.

For each shoulder, the three central-most coronal-oblique images relative to the humeral head were identified based on axial localizer images (Figure 1A). The RCT on each coronal-oblique image was manually segmented from the center of the humeral head to the greater tuberosity attachment since this is the location of the myotendinous junction in the majority of individuals (7) (Figure 1B). Care was also taken to include only areas of the tendon without surrounding bone or articular hyaline cartilage. The fibrocartilage regions near the enthesis were included in the region of interest (ROI). The manually segmented RCT on each image was automatically divided into six sub-segments, based on bursal-sided (superior) and articular-sided (inferior) halves as well as medial, middle, and lateral thirds of equal size (Figure 1C). In total, each shoulder had 18 anatomically distinct segments available for analysis (3 slices x 6 segments per slice). A Levenberg–Marquardt algorithm was employed for the non-linear least-squares fitting for T_1 and T_2 fitting as well as for the MT model. Two-pool UTE-Cones-MT modeling and parameter mapping were performed on the datasets as previously described (14,24). Image registration, segmentation, and analyses were performed in MATLAB (MathWorks, 2016b, Natick, MA) by a research fellow and all ROIs were reviewed by a musculoskeletal radiologist.

Statistical Analysis

Statistical analyses were performed with R software, version 2.10.1 (2009) (R Foundation for Statistical Computing, Vienna, Austria). Analyses were performed based on different

anatomic regions, including all segments (18 per shoulder) as well as the lateral-third segments (6 per shoulder) since the majority of RCT abnormalities occur in this region (25). The bursal-sided (9 per shoulder) and articular-sided segments (9 per shoulder) were also analyzed due to potential differences in these regions, as suggested in previous literature (26). The Shapiro–Wilk test was used to assess normality. Descriptive statistics were performed. For each imaging measure, the three groups (symptomatic shoulders, asymptomatic shoulders of patients, and control shoulders) were compared pairwise using a bootstrap-based comparison of means to adjust for within-subject dependence. Percent differences between groups were calculated based on the formula: |group 1 – group 2| / [(group 1 + group 2) / 2]. For symptomatic shoulders, Spearman's correlation was used to assess the relationship between all-segment MRI analyses and clinical scores (WORC and VAS). $P < 0.05$ was considered to represent statistically significant findings.

Results

Study Population and Clinical Data

Fifteen patients with unilateral shoulder pain met inclusion criteria. One study subject was excluded due to inability to complete the quantitative MRI protocol. 48 shoulders were scanned in total, including both shoulders from 14 unilaterally symptomatic subjects (10 males and 4 females, mean age of 35.8 ± 6.3) and both shoulders from 10 control subjects (5 males and 5 females, mean age of 28.6 ± 7.0).

The mean WORC percentage score was 31.8 ± 19.43% for symptomatic shoulders. The mean VAS score was 7.3 ± 1.64 for symptomatic shoulders and 0.0 ± 0 for both asymptomatic and control shoulders.

Quantitative MRI

Figures 2 and 3 show representative images, pixel maps, and fitting curves for MMF and T_2 results, respectively. Table 1 shows the mean MMF and T_2 values for the groups and Tables 2 and 3 show the pairwise comparisons between groups. For the analysis including all segments, the mean MMF values for symptomatic shoulders, asymptomatic shoulders of patients, and control individuals was 13.19 ± 2.44%, 12.88 ± 2.8%, and 14.06 ± 3.03%, respectively. The MMF values including all segments showed a percent difference of 6.39% between control and symptomatic shoulders (p=0.027), 8.76% between control shoulders and asymptomatic shoulders of patients (p=0.024), and no significant difference (p=0.540) between asymptomatic and symptomatic shoulders. For the analysis including all segments, the mean T_2 value for symptomatic shoulders, asymptomatic shoulders of patients, and control individuals was 21.24 ± 4.27 ms, 21.08 ± 4.39 ms, and 19.13 ± 3.42 ms, respectively. T_2 values showed a percent difference of 10.45% between control and symptomatic shoulders (p=0.006), 9.70% between control shoulders and asymptomatic shoulders of patients (p=0.003), and no significant differences between asymptomatic and symptomatic shoulders (p=0.91).

For the lateral tendon segments, mean MMF value for symptomatic shoulders, asymptomatic shoulders of patients, and control individuals was 14.33 ± 2.38%, 14.25 ± 2.43%, and 15.56

± 3.12%, respectively. MMF values for lateral segments showed a percent difference of 8.79% between control shoulders and asymptomatic shoulders of patients (p=0.04), a percent difference of 8.23% between control and symptomatic shoulders which was trend-level but did not reach statistical significance (p=0.07), and no significant difference between asymptomatic and symptomatic shoulders (p=0.87). The mean T_2 values of the lateral segments for symptomatic shoulders, asymptomatic shoulders of patients, and control individuals was 19.33 ± 4.38 ms, 20.15 ± 4.10 ms, and 19.30 ± 3.59 ms, respectively. No significant differences in T_2 were found between control and symptomatic shoulders (p=0.95), control shoulders and asymptomatic shoulders of patients (p=0.38), or between asymptomatic and symptomatic shoulders (p=0.38) in the lateral tendon segments.

For the bursal-sided segments of the rotator cuff tendon, MMF values for symptomatic shoulders, asymptomatic shoulders of patients, and controls individuals was 12.7 ± 2.66%, 12.13 ± 2.56%, and 13.13 ± 2.87%, respectively. MMF values for the bursal-sided segments showed a difference of 7.92% between control shoulders and asymptomatic shoulders of patients (p=0.044), but no significant differences between control and symptomatic shoulders (p=0.280) or between asymptomatic and symptomatic shoulders (p=0.420). The mean T_2 values for the bursal-sided segments of the rotator cuff tendon for symptomatic shoulders, asymptomatic shoulders of patients, and control individuals was 21.97 ± 4.18 ms, 22.54 ± 4.35 ms, and 20.58 ± 3.59 ms, respectively. T_2 values showed a difference of 9.18% between control shoulders and asymptomatic shoulders of patients (p=0.021), but no significant differences between control and symptomatic shoulders (p=0.120), or between asymptomatic and symptomatic shoulders (p=0.660).

For the articular-sided segments of the rotator cuff tendon, MMF values for symptomatic shoulders, asymptomatic shoulders of patients, and controls individuals was 13.67 ± 2.11%, 13.63 ± 2.80%, and 14.98 ± 2.90%, respectively. MMF values showed a difference of 9.14% between control and symptomatic shoulders (p=0.001), 9.44% between control shoulders and asymptomatic shoulders of patients (p=0.037), but no significant differences between asymptomatic and symptomatic shoulders (p=0.950). The mean T_2 values of the articular-sided segments for symptomatic shoulders, asymptomatic shoulders of patients, and control individuals was 20.5 ± 4.24 ms, 19.62 ± 3.94 ms, and 17.67 ± 3.59 ms, respectively. T_2 values showed a difference of 14.83% between control and symptomatic shoulders (p=0.001), 10.46% between control shoulders and asymptomatic shoulders of patients (p=0.002), and no significant differences between asymptomatic and symptomatic shoulders (p=0.400).

No significant correlations were found between quantitative MRI and WORC scores (p=0.9 for MMF and p=0.7 for T_2) or between quantitative MRI and visual analog scale scores (p=0.98 for MMF and p=0.12 for T_2).

Discussion

In our study, we used quantitative MRI to assess the bilateral RCTs of patients presenting with unilateral symptomatic tendinopathy and in asymptomatic controls. We found significant differences in both MMF and T_2 values between symptomatic and control RCTs

when all-segments and articular-sided segments were analyzed. Notably, differences between asymptomatic RCTs in patients and control RCTs were also found, including MMF in all anatomic regions analyzed and T_2 in all anatomic regions analyzed except the lateral segments. No significant differences in MMF or T_2 were seen between ipsilateral symptomatic and contralateral asymptomatic RCTs in patients.

MMF and T_2 have been previously shown to be sensitive to RCT tendinosis in *ex vivo* studies using histologic and biochemical reference standards (14,27). In our study, the articular-sided segments showed the largest percent differences in both MMF (9.14%) and T_2 (14.83%) between control and symptomatic RCTs, indicating degeneration. These findings can be explained by the results of Nakajima et al., who demonstrated that the articular side of the cuff was predilectively prone to pathology and rupture compared with the bursal side of the tendon due to its composition, which included tendon, ligament, and joint capsule, which was distinct when compared with the more tendinous bursal-side of the RCT (26).

Although T_2 is sensitive to and potentially confounded by the magic angle effect, our results demonstrate that, when assessing all 18 RCT segments, it remained an excellent measure which showed differences between symptomatic patients and control subjects. MMF, a magic-angle insensitive measure, was also useful for this purpose when assessing all 18 RCT segments. However, when analyzing the lateral-only segments, MMF but not T_2 revealed differences between patients and volunteers. One explanation may be that, for this particular region, the tendon fibers usually course near the magic angle (54.78°). Prolonged T_2 values from the normal tendons as a consequence of the magic angle effect may approximate the prolonged T_2 values from pathologically degenerated tendons. This explanation is supported by results from Zhu et al. who also found decreased sensitivity of T_2 in distinguishing between normal and tendinotic groups at the magic angle, but not other angles (14).

Significant differences in quantitative MRI measures were found between asymptomatic RCTs in patient and control RCTs, with percent differences greater in almost all instances than in those found between symptomatic and control RCTs. These findings suggest that patients with unilateral, symptomatic RCT tendinopathy may have similar degeneration in their contralateral, asymptomatic RCT. Our findings are consistent with numerous preceding reports which found that patients treated for RCT tears in one shoulder had significantly higher risk of having tears in the other shoulder, even when asymptomatic (4,28,29). Furthermore, we did not find any significant correlation between degree of tendinosis and WORC or visual analog scale, which is consistent with reports from previous authors showing that RCT tear size did not correlate with WORC (30) or visual analog scale (3). However, it is still clear that the relationship between tendon integrity, function, and symptoms warrants additional study, since there is evidence that asymptomatic RCT pathology is more likely to become symptomatic over time with corresponding decreased function (5). Furthermore, systematic reviews have found inconsistent findings regarding patient-reported outcomes, strength, range of motion, and kinematics in individuals with asymptomatic RCTs (5).

Limitations

There were some limitations of our study that should be acknowledged. First is the limited study size. Although we found significant differences between symptomatic patients and control subjects, a larger number of participants may have been helpful for better delineation of the trend-level changes in the lateral segments. Second, because our study did not include surgical or histopathologic correlation, we are unable to entirely exclude tendinosis in the control group. Third, caution should be exercised when extrapolating our results to other study groups since we used strict exclusion criteria; notably, we only included patients with unilateral symptoms and whose MR imaging showed no RCT tears or other non-RCT pathologies. Fourth, the UTE-Cones-MT sequence is not yet commercially available and future multi-center studies will be needed to increase the generalizability of our results. However, utilization of this sequence only requires software installation without hardware modifications and UTE sequences with various k-space trajectories and preparations have been successfully employed on MRI machines from every major vendor. Fifth, manual segmentation of the rotator cuff was performed by a single reader and therefore reproducibility was not evaluated. In future studies alternate strategies may be useful, including segmentation by multiple readers as well as use of deep learning-based segmentation algorithms.

Conclusion

We used quantitative MMF and T_2 measures to assess cuff tendinosis in both shoulders in symptomatic and control groups. Symptomatic RCTs showed significantly lower MMF and higher T_2 values compared with control RCTs. MMF may be more sensitive to pathology compared with T_2, particularly for evaluation of the lateral RCT which courses near the magic angle. In patients with unilateral RCT pain, the contralateral shoulder can demonstrate asymptomatic tendinopathy which can be assessed using MMF or T_2.

Acknowledgments

Grant Support: The authors gratefully acknowledge grant support from the Veterans Affairs (Merit Awards I01CX001388 and I01RX002604) and the NIH (1R01AR075825, 5R21AR0734965, 5R01AR062581, and 5R01NS092650).

References

1. Kramer EJ, Bodendorfer BM, Laron D, et al. Evaluation of cartilage degeneration in a rat model of rotator cuff tear arthropathy. Journal of shoulder and elbow surgery / American Shoulder and Elbow Surgeons [et al.] 2013;22(12):1702–1709.
2. Shanahan EM, Sladek R. Shoulder pain at the workplace. Best practice & research Clinical rheumatology 2011;25(1):59–68. [PubMed: 21663850]
3. Dunn WR, Kuhn JE, Sanders R, et al. Symptoms of pain do not correlate with rotator cuff tear severity: a cross-sectional study of 393 patients with a symptomatic atraumatic full-thickness rotator cuff tear. J Bone Joint Surg Am 2014;96(10):793–800. [PubMed: 24875019]
4. Ro KH, Park JH, Lee SH, Song DI, Jeong HJ, Jeong WK. Status of the contralateral rotator cuff in patients undergoing rotator cuff repair. Am J Sports Med 2015;43(5):1091–1098. [PubMed: 25740834]
5. Lawrence RL, Moutzouros V, Bey MJ. Asymptomatic Rotator Cuff Tears. JBJS Rev 2019;7(6):e9.

6. Stoller DW, Stoller DW. Magnetic resonance imaging in orthopaedics and sports medicine. Philadelphia: Lippincott Williams & Wilkins: 2007.
7. Neumann CH, Holt RG, Steinbach LS, Jahnke AH Jr., Petersen SA. MR imaging of the shoulder: appearance of the supraspinatus tendon in asymptomatic volunteers. AJR Am J Roentgenol 1992;158(6):1281–1287. [PubMed: 1590124]
8. Robertson PL, Schweitzer ME, Mitchell DG, et al. Rotator cuff disorders: interobserver and intraobserver variation in diagnosis with MR imaging. Radiology 1995;194(3):831–835. [PubMed: 7862988]
9. Roy JS, Braen C, Leblond J, et al. Diagnostic accuracy of ultrasonography, MRI and MR arthrography in the characterisation of rotator cuff disorders: a systematic review and meta-analysis. Br J Sports Med 2015;49(20):1316–1328. [PubMed: 25677796]
10. Sein ML, Walton J, Linklater J, et al. Reliability of MRI assessment of supraspinatus tendinopathy. Br J Sports Med 2007;41(8):e9. [PubMed: 17289860]
11. Anz AW, Lucas EP, Fitzcharles EK, Surowiec RK, Millett PJ, Ho CP. MRI T2 mapping of the asymptomatic supraspinatus tendon by age and imaging plane using clinically relevant subregions. European journal of radiology 2014;83(5):801–805. [PubMed: 24613548]
12. Ganal E, Ho CP, Wilson KJ, et al. Quantitative MRI characterization of arthroscopically verified supraspinatus pathology: comparison of tendon tears, tendinosis and asymptomatic supraspinatus tendons with T2 mapping. Knee surgery, sports traumatology, arthroscopy : official journal of the ESSKA 2016;24(7):2216–2224.
13. Krepkin K, Bruno M, Raya JG, Adler RS, Gyftopoulos S. Quantitative assessment of the supraspinatus tendon on MRI using T2/T2* mapping and shear-wave ultrasound elastography: a pilot study. Skeletal Radiol 2017;46(2):191–199. [PubMed: 27896400]
14. Zhu Y, Cheng X, Ma Y, et al. Rotator cuff tendon assessment using magic-angle insensitive 3D ultrashort echo time cones magnetization transfer (UTE-Cones-MT) imaging and modeling with histological correlation. J Magn Reson Imaging 2018;48(1):160–168. [PubMed: 29219218]
15. Chang EY, Du J, Chung CB. UTE imaging in the musculoskeletal system. J Magn Reson Imaging 2015;41(4):870–883. [PubMed: 25045018]
16. Kirkley A, Alvarez C, Griffin S. The development and evaluation of a disease-specific quality-of-life questionnaire for disorders of the rotator cuff: The Western Ontario Rotator Cuff Index. Clin J Sport Med 2003;13(2):84–92. [PubMed: 12629425]
17. Ma YJ, Chang EY, Carl M, Du J. Quantitative magnetization transfer ultrashort echo time imaging using a time-efficient 3D multispoke Cones sequence. Magn Reson Med 2018;79(2):692–700. [PubMed: 28470838]
18. Ma YJ, Zhu Y, Lu X, Carl M, Chang EY, Du J. Short T2 imaging using a 3D double adiabatic inversion recovery prepared ultrashort echo time cones (3D DIR-UTE-Cones) sequence. Magn Reson Med 2018;79(5):2555–2563. [PubMed: 28913879]
19. Ma YJ, Lu X, Carl M, et al. Accurate T1 mapping of short T2 tissues using a three-dimensional ultrashort echo time cones actual flip angle imaging-variable repetition time (3D UTE-Cones AFI-VTR) method. Magn Reson Med 2018;80(2):598–608. [PubMed: 29314235]
20. Ma YJ, Zhao W, Wan L, et al. Whole knee joint T1 values measured in vivo at 3T by combined 3D ultrashort echo time cones actual flip angle and variable flip angle methods. Magn Reson Med 2019;81(3):1634–1644. [PubMed: 30443925]
21. Raman J, Macdermid JC. Western Ontario Rotator Cuff Index. J Physiother 2012;58(3):201. [PubMed: 22884191]
22. Periaswamy S, Farid H. Elastic registration in the presence of intensity variations. IEEE Trans Med Imaging 2003;22(7):865–874. [PubMed: 12906240]
23. Klein S, Staring M, Murphy K, Viergever MA, Pluim JP. elastix: a toolbox for intensity-based medical image registration. IEEE Trans Med Imaging 2010;29(1):196–205. [PubMed: 19923044]
24. Ma YJ, Shao H, Du J, Chang EY. Ultrashort echo time magnetization transfer (UTE-MT) imaging and modeling: magic angle independent biomarkers of tissue properties. NMR Biomed 2016;29(11):1546–1552. [PubMed: 27599046]

25. Kim HM, Dahiya N, Teefey SA, et al. Location and initiation of degenerative rotator cuff tears: an analysis of three hundred and sixty shoulders. J Bone Joint Surg Am 2010;92(5):1088–1096. [PubMed: 20439653]

26. Nakajima T, Rokuuma N, Hamada K, Tomatsu T, Fukuda H. Histologic and biomechanical characteristics of the supraspinatus tendon: Reference to rotator cuff tearing. Journal of shoulder and elbow surgery / American Shoulder and Elbow Surgeons [et al.] 1994;3(2):79–87.

27. Guo T, Ma YJ, High RA, et al. Assessment of an in vitro model of rotator cuff degeneration using quantitative magnetic resonance and ultrasound imaging with biochemical and histological correlation. European journal of radiology 2019;121:108706. [PubMed: 31655315]

28. Liem D, Buschmann VE, Schmidt C, et al. The prevalence of rotator cuff tears: is the contralateral shoulder at risk? Am J Sports Med 2014;42(4):826–830. [PubMed: 24500916]

29. Ranebo MC, Bjornsson Hallgren HC, Adolfsson LE. Patients with a long-standing cuff tear in one shoulder have high rates of contralateral cuff tears: a study of patients with arthroscopically verified cuff tears 22 years ago. Journal of shoulder and elbow surgery / American Shoulder and Elbow Surgeons [et al.] 2018;27(3):e68–e74.

30. Harris JD, Pedroza A, Jones GL, Group MS. Predictors of pain and function in patients with symptomatic, atraumatic full-thickness rotator cuff tears: a time-zero analysis of a prospective patient cohort enrolled in a structured physical therapy program. Am J Sports Med 2012;40(2):359–366. [PubMed: 22095706]

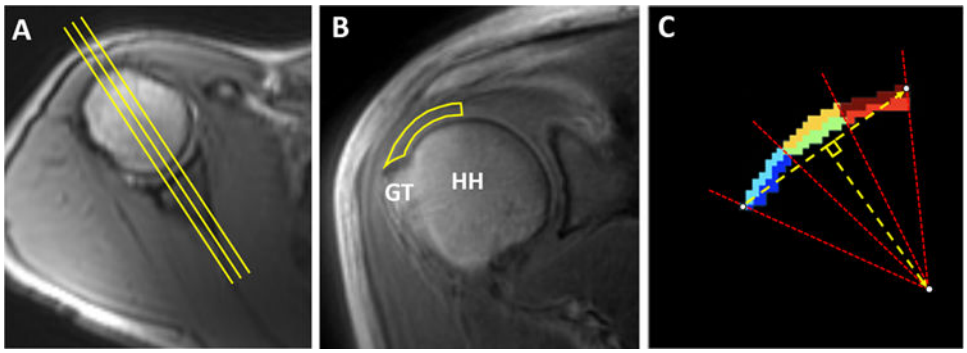

Figure 1.

Methodology for segmentation. (A) Using an axial localizer image, three central-most coronal-oblique images relative to the humeral head were identified (yellow lines). (B) Coronal-oblique image demonstrates manually segmented RCT from the center of the humeral head to the greater tuberosity attachment. (C) For each manually segmented region on each slice, six subsegments of equal size were automatically divided based on bursal-sided (dark red, orange, and light blue) and articular-sided (red, green, and dark blue) halves as well as medial (dark red and red), middle (orange and green), and lateral thirds (light blue and blue). HH: humeral head, GT: greater tuberosity.

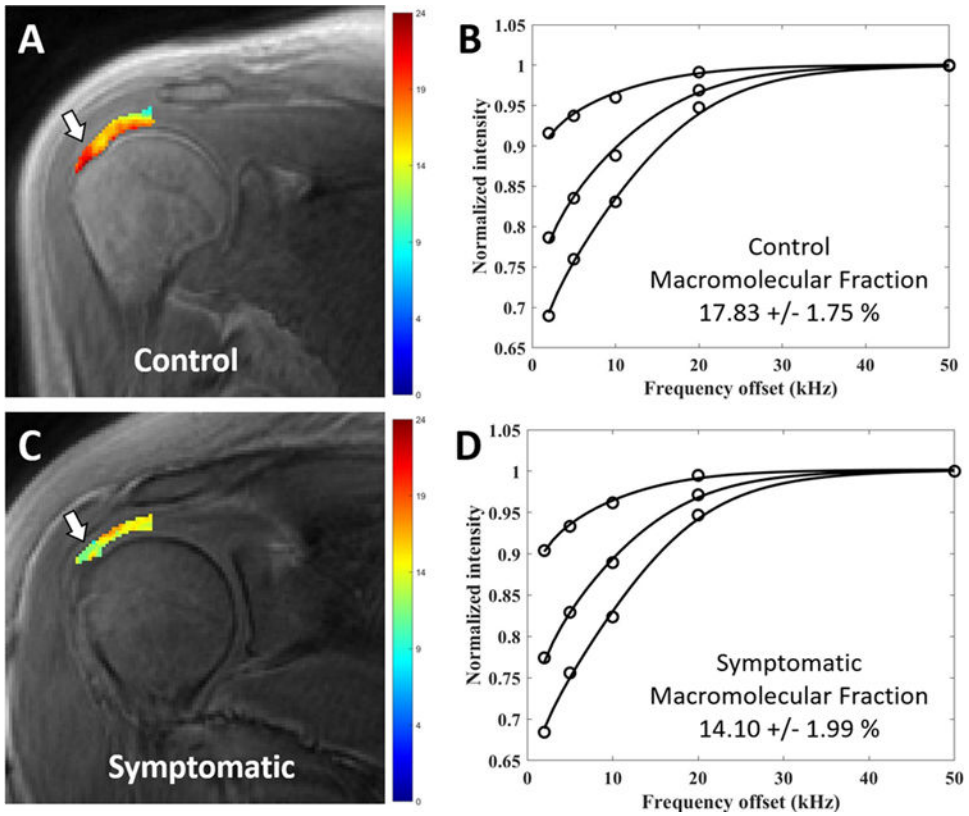

Figure 2.

Coronal oblique UTE-Cones-MT images with pixel maps from two-pool MT modeling for the superior rotator cuff tendon and fitting curves. (A) Pixel map overlay from a 31-year-old control subject demonstrates region of interest used for tendon analysis, from which six segments were delineated. (B) Fitting curve from the entire ROI, including all six segments on this slice, shows excellent fit with mean macromolecular fraction of 17.83%. (C) Pixel map overlay from a 29-year-old symptomatic patient demonstrates areas of visibly lower MMF values compared with (A) (white arrows). (D) Fitting curve from the entire ROI, including all six segments on this slice, shows excellent fit with mean macromolecular fraction of 14.10%.

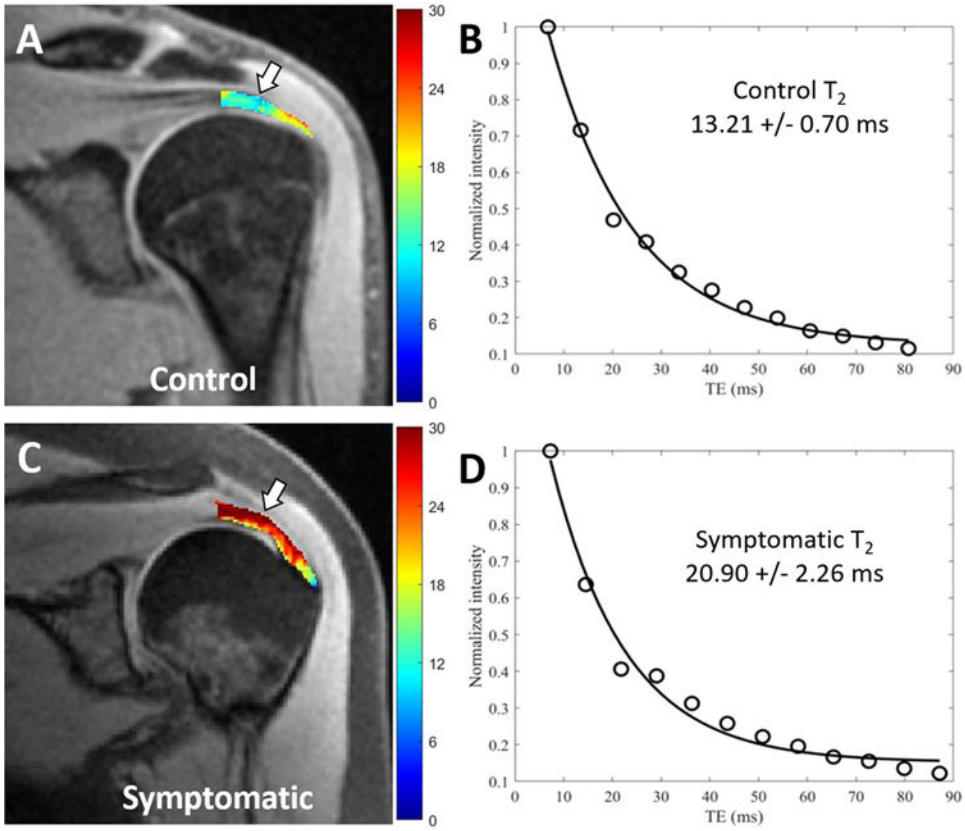

Figure 3.

Coronal oblique spin echo images with pixel maps from single component T_2 analysis for the superior rotator cuff tendon and fitting curves. (A) Pixel map overlay from a 24-year-old control subject demonstrates region of interest (ROI) used for tendon analysis, from which six segments were delineated. (B) Fitting curve on the entire ROI, including all six segments on this slice, shows a T_2 value of 13.21 ms. (C) Pixel map overlay from a 42-year-old symptomatic patient demonstrates elevated T_2 values compared with (A) (white arrows). (D) Fitting curve from the entire ROI, including all six segments on this slice, shows a T_2 value of 20.90 ms.

Table 1.

Macromolecular Fraction (MMF) & T_2 Values of Each Group for Each Corresponding Region.

Group	Region	MMF (%)	T_2 (ms)
Symptomatic	All segments	13.19 ± 2.44	21.24 ± 4.27
Asymptomatic	All segments	12.88 ± 2.80	21.08 ± 4.39
Control	All segments	14.06 ± 3.03	19.13 ± 3.42
Symptomatic	Lateral segments	14.33 ± 2.38	19.33 ± 4.38
Asymptomatic	Lateral segments	14.25 ± 2.43	20.15 ± 4.10
Control	Lateral segments	15.56 ± 3.12	19.30 ± 3.59
Symptomatic	Bursal-sided segments	12.70 ± 2.66	21.97 ± 4.18
Asymptomatic	Bursal-sided segments	12.13 ± 2.58	22.56 ± 4.35
Control	Bursal-sided segments	13.13 ± 2.87	20.58 ± 3.59
Symptomatic	Articular-sided segments	13.67 ± 2.20	20.50 ± 4.25
Asymptomatic	Articular-sided segments	13.63 ± 2.80	19.62 ± 3.94
Control	Articular-sided segments	14.98 ± 2.90	17.67 ± 2.52

Mean ± standard deviation values are shown.

Table 2.

Pairwise Comparisons of Macromolecular Fraction (MMF) Between Groups for Each Corresponding Region.

Group	Region	MMF Mean Difference, [95% Confidence Interval] (%)	p-value	MMF Difference[1] (%)
Control - Symptomatic	All segments	0.87, [0.09 – 1.84]	**0.027**	6.39
Control - Asymptomatic	All segments	1.18, [0.20 – 2.63]	**0.024**	8.76
Asymptomatic - Symptomatic	All segments	−0.31, [−1.27 – 0.70]	0.540	2.38
Control - Symptomatic	Lateral segments	1.23, [−0.10 – 2.58]	**0.027**	8.23
Control - Asymptomatic	Lateral segments	1.31, [0.06 – 2.45]	**0.040**	8.79
Asymptomatic - Symptomatic	Lateral segments	−0.08, [−1.40 – 1.12]	0.870	0.56
Control - Symptomatic	Bursal-sided segments	0.43, [−0.43 – 1.67]	0.280	6.39
Control - Asymptomatic	Bursal-sided segments	1.01, [0 – 2.02]	**0.044**	3.33
Asymptomatic - Symptomatic	Bursal-sided segments	−0.58, [−1.53 – 0.74]	0.420	7.92
Control - Symptomatic	Articular-sided segments	1.31, [0.54 – 2.23]	**0.001**	9.14
Control - Asymptomatic	Articular-sided segments	1.35, [0.07 – 2.44]	**0.037**	9.44
Asymptomatic - Symptomatic	Articular-sided segments	−0.04, [−0.99 – 1.23]	0.950	0.30

[1]Percent difference = |group 1 – group 2| / [(group 1 + group 2) / 2]

Table 3.

Pairwise Comparisons of T_2 Between Groups for Each Corresponding Region.

Group	Region	T_2 Mean Difference, [95% Confidence Interval] (%)	p-value	T_2 Difference[1] (%)
Control - Symptomatic	All segments	−2.11, [−3.72 - −0.63]	**0.006**	10.45
Control - Asymptomatic	All segments	−1.95, [−3.83 – −0.52]	**0.003**	9.70
Asymptomatic - Symptomatic	All segments	−0.15, [−1.98 – 2.19]	0.910	0.76
Control - Symptomatic	Lateral segments	−0.03, [−2.32 – 1.61]	0.950	0.16
Control - Asymptomatic	Lateral segments	−0.85, [−2.81 – 0.97]	0.380	4.31
Asymptomatic - Symptomatic	Lateral segments	0.82, [−1.08 – 2.57]	0.380	4.15
Control - Symptomatic	Bursal-sided segments	−1.39, [−3.63 – 0.30]	0.120	6.53
Control - Asymptomatic	Bursal-sided segments	−1.96, [−4.13 – −0.26]	**0.021**	9.18
Asymptomatic - Symptomatic	Bursal-sided segments	0.58, [−2.00 – 3.05]	0.660	2.65
Control - Symptomatic	Articular-sided segments	−2.83, [−4.39 – −1.34]	**0.001**	14.83
Control - Asymptomatic	Articular-sided segments	−1.95, [−3.90 – −0.7]	**0.002**	10.46
Asymptomatic - Symptomatic	Articular-sided segments	−0.88, [−2.90 – 1.20]	0.400	4.39

[1]Percent difference = |group 1 – group 2| / [(group 1 + group 2) / 2]